Fermions in a massive vector background: a cosmological study

Abel Muñoz Navarro, Advisors: Adrià Gómez Valent, Jordi Salvadó Serra

Facultat de Física, Universitat de Barcelona, Martí i Franquès 1, 08028 Barcelona, Spain.

E-mail: abelmunoznavarro@gmail.com

Abstract: We propose a model of interactions between fermions and a massive vector field. The mass of this bosonic mediator determines the effective range of the derived forces, spanning scales from cosmological to galactic or even smaller. An action for this interaction model is postulated, where the fermionic candidates are neutrinos and dark matter particles. From it, we derive the classical solutions for the vector field, and we seek the modifications produced by the inclusion of such a vectorial background in the equations of motion of the fermions. Microphysical properties, including production rates, scattering cross-sections, and decay widths of both vector and Dirac particles, are also derived. These rates enable us to track the non-trivial evolution of the particle populations during the expansion of the Universe. By systematically proving the parameter space, we find that specific physical observables impose constraints on each region. To conclude, three particular scenarios with non-standard contributions from our interaction to the Λ-Cold Dark Matter model are discussed: the rise on the effective number of neutrino species, the abundances of particles produced during the Big Bang Nucleosynthesis, and the effects of classical solutions on the equation of state of the early universe fluid.

En aquesta tesi proposem un model d'interaccions entre fermions i un camp vectorial massiu. L'abast de les interaccions que en resulten dependrà de l'escala de la massa del mediador, podent aquestes abarcar des de règims cosmològics fins a galàctics o encara inferiors. Plantegem el fonament teòric del model des de primers principis considerant com a candidats fermiònics per la interacció els neutrins i la matèria fosca. En derivem les solucions clàssiques del camp vectorial que són compatibles amb el Principi Cosmològic, trobem les modificacions en les equacions fonamentals dels fermions, així com els ritmes de producció, interacció i decaïment de les partícules involucrades en els processos. Aquests ens permeten seguir l'evolució no trivial de les poblacions de les partícules durant l'expansió de l'Univers. Realitzant una exploració sistemàtica de l'espai de paràmetres hem identificat quins observables entren en joc a l'hora de constrènyer el model amb mesures experimentals a cada regió. Finalment, estudiem tres casos particulars en què s'observen contribucions fora del model estàndard cosmològic en el nombre efectiu de neutrins, les abundàncies durant la nucleosíntesi primordial i l'equació d'estat de l'univers en les seves etapes inicials.

Keywords: cosmology, elementary particles, quantum field theory, particle physics, theoretical physics

Contents

1 Introduction

Modern cosmology and particle physics are built upon two of the most successful theoretical frameworks in physics: the Λ-Cold Dark Matter (ΛCDM) model [1] and the Standard Model of Particle Physics (SM). Even if the vast majority of the predictions of these theories have been extensively confirmed by experimental and observational data [2, 3], they face significant challenges that hint at phenomena whose understanding is beyond their current formulations. The ΛCDM model provides a robust description of the large-scale structure and evolution of the universe, yet it remains opaque in giving an intuitive understanding of cosmological content. The final nature of dark matter (DM) and dark energy, as well as the origin of the matter-antimatter asymmetry, are fundamental problems of the theory. Similarly, the SM depicts the known elementary particles and the interactions among them, but lacks an explanation for neutrino oscillations, as their masses are not included in the model, and misses a candidate for DM. One intriguing connection between cosmology and particle physics lies precisely in the role of neutrinos. While terrestrial experiments constrain an upper limit on its mass, this value is significantly higher than cosmological estimates. Since neutrinos interact weakly, cosmological observables remain an open window for the discovery of their properties, including constraining their absolute mass, scale and hierarchy. Examples of such observables are the cosmic microwave

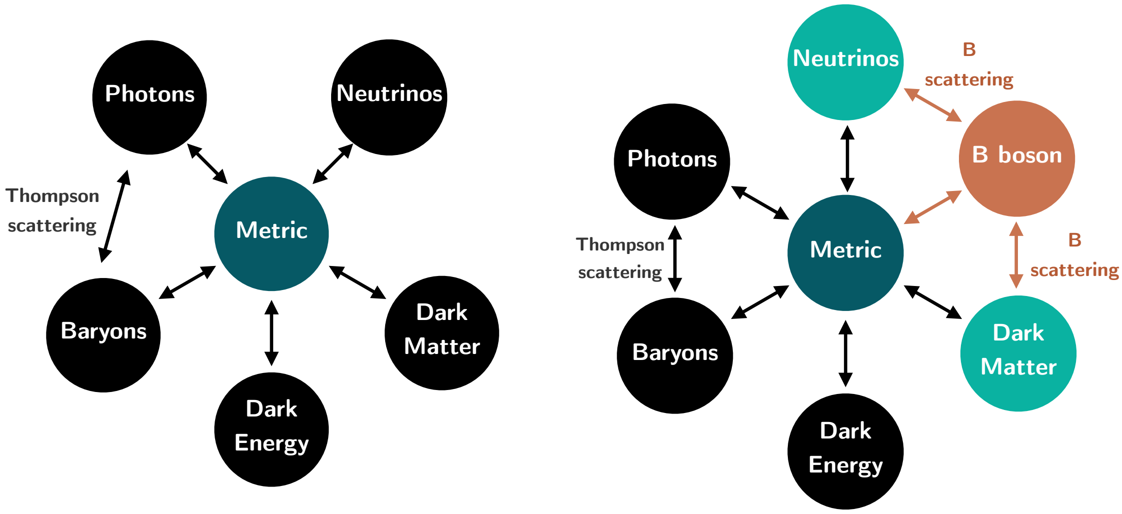

Figure 1. Left: SM species and their interactions. Right: particles and interactions of the proposed model in this thesis. A massive vector boson is added, which can be coupled to neutrinos and/or dark matter.

background (CMB), large-scale structure (LSS), and Big Bang nucleosynthesis (BBN) [4]. These sources of data allow us to characterise the dark sector and also to probe non-trivial couplings between this sector and ordinary fermionic matter, and specifically cosmological neutrinos. This kind of interaction stamps observable imprints in the energy distribution of the universe, as well as in the growth of cosmic structures, offering an exotic point of view of both neutrino physics and the nature of DM.

In this work, we propose the interaction of a fermionic particle with a massive vector boson, the B. Depending on the mass scale, this interaction mediates long-range forces acting across cosmological, galactic or even small scales. Despite this, we are interested in scenarios in which these forces do not compete with gravity on large scales, but introduce new effects on smaller ones. The foundation of our proposal lies in the existence of classical solutions of the vectorial field, consistent with both the background symmetries and the equations of motion. In previous studies, the scalar-fermionic scenario has been explored [5], and such couplings have led to non-trivial modifications in the equation of state, altering the energy density and pressure distributions, on both background cosmology, i.e. respecting the homogeneity and isotropy assumptions, and perturbations (beyond this hypotheses). The main effect of considering a classical scalar field interaction is conferring an additional mass to the fermions. In the coming sections, we will prove that the effect of the classical vectorial field solutions will bear no resemblance at all to this effect; instead, a global energy sourcing in the fermionic field will rise. Our model is parametrised by the fundamental quantities, the mass of the boson M_B, the coupling g, and the present value of fermion-antifermion asymmetry Δn_f^0, which determines the current charge of the universe under this new vectorial field. Different non-trivial predictions on effects in the cosmological observables will appear depending on the values of these parameters. As a first approach, this work considers three distinguished sets of parameter values that produce three different scenarios for physical observables as the neutrino effective number of particles, the abundances during BBN production and the energy distribution of the species. Further research will constrain with state-of-the-art cosmological data [6, 7] the best fit parameters for this model, and the effect on ΛCDM.

This thesis is structured as follows. In section 2.1, we introduce our formalism for a generic interaction between a fermion and a vector in a cosmological context. The action is presented in 2.2, and the consistency of its proposal is discussed. The classical solutions of the B field, as well as the modifications in the fermionic equations of motion and solutions, are computed in sections 2.3 and 2.4, respectively. In section 2.5, we explain how the classical solutions, as well as the thermal components of each species, contribute to the total energy density and pressure. In 2.6, it is explained how the rates of scattering processes can tell us about the evolution of the distribution functions that characterise the energy content of the universe. Three differentiated scenarios are presented in section 3, in which the coupling plays distinct roles when imprinting the cosmological observables. Finally, we summarise our results in section 4.

2 Theoretical Framework

2.1 Formalism

When studying cosmology, choosing a metric that encapsulates the effects of gravity according to general relativity is essential. The universe appears homogeneous and isotropic on large scales, and it is the standard approach to promote these observations to an assumption, the so-called Cosmological Principle (CP), from which a metric can be derived. The Friedmann-Lemaître-Robertson-Walker (FRLW) metric is consistent with the symmetries imposed by the CP, and allows us to decompose space-time into completely homogeneous and isotropic hypersurfaces of constant cosmic time t. In this thesis, we opt for the conformal form of the FRLW, with the line element given by:

$$ds^2 = a^2(\eta)\left(-d\eta^2 + dx^i dx^j\,\delta_{ij}\right)\,, \tag{2.1}$$

where $dt = a(\eta)d\eta$, with η the conformal time, x^i the comoving spatial coordinates and a the scale factor that parametrises the expansion of the universe. The convention $c = \hbar = k_B = 1$ will be used throughout this work, as well as the dot as the derivative with respect to the cosmic time. We also use $' \equiv d/d\eta$ and $\nabla^2 \equiv \partial_i\partial^i$. The Hubble parameter is defined as $H = \dot{a}/a$, and represents the rate at which the universe is expanding.

In differential geometry, the Christoffel symbols $\Gamma^\lambda_{\mu\nu}$ are defined in terms of the metric tensor and its derivatives. They allow us to compare vectors at different points of space-time by defining in a proper way the parallel transport of a vector and the covariant derivative compatible with the metric. They can be computed as:

$$\Gamma^\lambda_{\mu\nu} = \frac{1}{2}g^{\lambda\sigma}\left(\partial_\mu g_{\nu\sigma} + \partial_\nu g_{\mu\sigma} - \partial_\sigma g_{\mu\nu}\right),$$

where $g_{\mu\nu}$ is the metric tensor. For the conformal FLRW metric, they reduce to the non-zero components:

$$\Gamma^0_{00} = \frac{a'}{a}, \quad \Gamma^0_{ij} = \frac{a'}{a}\delta_{ij}, \quad \Gamma^i_{0j} = \Gamma^i_{j0} = \frac{a'}{a}\delta^i_j\,. \tag{2.2}$$

Other geometrical quantities can be extracted from them: the Riemann curvature tensor $R^{\lambda}{}_{\mu\nu\sigma} = \partial_\nu \Gamma^{\lambda}{}_{\mu\sigma} + \Gamma^{\rho}{}_{\mu\sigma} \Gamma^{\lambda}{}_{\rho\nu} - (\nu \leftrightarrow \sigma)$, the Ricci tensor $R_{\mu\nu} = R^{\lambda}{}_{\mu\lambda\nu}$, and the Ricci scalar $R = g^{\mu\nu} R_{\mu\nu}$.

Matter fields must be coupled to the geometry of curved spacetime in a way that preserves general covariance. Scalar and vector fields can be formulated in terms of coordinate-based tensors, as they transform like tensors under coordinate changes. Conversely, fermionic fields transform under local Lorentz transformations, and not general coordinate transformations [8]. Therefore, to accommodate spinors in curved spacetime, it is convenient to introduce the tetrad e^a_μ, which consists of a set of four linearly independent vector fields defined at every point in space-time. We also introduce a generalised set of gamma matrices that fulfil the usual Clifford Algebra ($\{\underline{\gamma}^\mu, \underline{\gamma}^\nu\} = -2g^{\mu\nu}$). They are defined as follows:

$$g_{\mu\nu}(x) \equiv \eta_{ab}\, e^a_\mu(x)\, e^b_\nu(x)\,, \quad \underline{\gamma}^\mu(x) \equiv e^\mu_a(x)\gamma^a\,, \tag{2.3}$$

thus, in a FLRW universe they reduce to

$$e^\mu_\nu = \frac{1}{a}\delta^\mu_\nu\,, \quad \underline{\gamma}^\mu = \frac{1}{a}\gamma^\mu. \tag{2.4}$$

They allow us to define the covariant derivative of the Dirac field $\nabla_\mu = \partial_\mu - \Gamma_\mu$ in terms of the spin connection Γ_μ, which fulfils the following equation [9]:

$$\left[\Gamma_\nu, \underline{\gamma}^\mu\right] = \frac{\partial \underline{\gamma}^\mu}{\partial x^\nu} + \Gamma^\mu_{\nu\rho}\underline{\gamma}^\rho\,. \tag{2.5}$$

In this way, the curved-space gamma matrices are defined to be covariantly constant over the spacetime manifold, $\nabla_\nu \underline{\gamma}^\mu = 0$. Using the Christoffel symbols from equation (2.2), we find that in a FLRW universe the spinorial connection is

$$\Gamma_0 = 0\,, \quad \Gamma_i = -\frac{a'}{2a}\gamma_i\gamma_0\,. \tag{2.6}$$

To conclude with the conventions, the Dirac representation of gamma matrices will be used,

$$\gamma^0 = \begin{pmatrix} I & 0 \\ 0 & -I \end{pmatrix}, \quad \gamma^i = \begin{pmatrix} 0 & \sigma^i \\ -\sigma^i & 0 \end{pmatrix}, \quad (i = 1, 2, 3)\,, \tag{2.7}$$

with σ^i the Pauli matrices.

2.2 The model for the interacting fermion-vector system

As discussed in the introduction, the interaction between a fermionic family and a massive vector boson will be studied. The following action is proposed for this interacting system,

$$S \supset \int d^4x \sqrt{-\mathcal{G}} \left[-\frac{1}{4}B_{\mu\nu}B^{\mu\nu} - \frac{1}{2}M_B^2 B_\mu B^\mu - \frac{i}{2}\left(\bar{\psi}\underline{\gamma}^\mu D_\mu \psi - D^*_\mu \bar{\psi}\underline{\gamma}^\mu \psi\right) - m\bar{\psi}\psi \right], \tag{2.8}$$

where ψ and B^μ correspond to the fermionic and vector fields, respectively, the field strength is given by $B_{\mu\nu} = \nabla_\mu B_\nu - \nabla_\nu B_\mu$, and D_μ contains the covariant derivative and the coupling, $D_\mu = \nabla_\mu + igB_\mu$.

The presence of the mass term for the Proca-type field breaks gauge invariance, and, as we will encounter in the following sections, including this term at arbitrarily high energies would violate unitarity. Therefore, B's mass must be given by some mechanism. The standard proposal consists of considering the coupling with a scalar field that acquires a vacuum expectation value at some energy scale. For energies of the particles below this scale, some degree of freedom of the scalar gets eaten by the vector boson, and it gets mass; effectively, our boson can be treated as a massive particle. While massive, the vector boson acquires an additional longitudinal mode and thus the internal degrees of freedom, given by the number of independent polarisations, is $\mathfrak{g}_B = 3$.

In the action (2.8), a generic fermion is considered. This is because two interesting physical scenarios can be modelled: the coupling with neutrinos or with fermionic dark matter. As a first approach, neutrinos are considered Dirac fermions, with both left and right-handed components. This allows us to learn about the physical consequences of this coupling and discover how cosmological observables can constrain the parameter space of the model in the rich neutrino-vector interactive scenario. However, the nature of such right-handed particles and the possible connections with the mechanism that gives mass to the vector field are left as further research to be solved and implemented in the model, in the future.

All the pieces that are contained in the action and do not appear in (2.8) correspond to the Einstein-Hilbert term and the fields of the SM particles, minimally coupled with gravity through the metric determinant. Their contribution is taken into account through their energy density and pressure, sourcing the gravitational field. When studying background cosmology, it is typically assumed that the energy density and pressure correspond to those of a perfect fluid, which dilutes as the universe expands. An ideal fluid of non-interacting relativistic particles has an energy density that dilutes as $\rho_\mathrm{r} \propto a^{-4}$ with equation of state parameter $\omega_\mathrm{r} \equiv P_\mathrm{r}/\rho_\mathrm{r} = 1/3$, where P_r is its pressure; and for non-relativistic matter particles $\rho_\mathrm{n.r.} \propto a^{-3}$ and $\omega_\mathrm{n.r.} = 0$. These expressions can be used to characterise matter when interactions are negligible over the expansion of the universe. Before this condition is fulfilled, the interactions between families demanded a different approach. A possibility is considering the evolution of the fluid as a function of the temperature, as it will be presented in the following sections.

The objective of this thesis is to solve the non-trivial evolution of the fermionic and Proca-like fluids of particles during the universe expansion. Now we have a starting point, from the action (2.8), we can extract both macro and micro physical information. In the following sections, we will explain how the classical equations of motion can be obtained, as well as the scattering rates of processes between them, which will determine the thermodynamic behaviour.

2.3 Classical solutions of the vectorial field

Extremizing the action (2.8) with respect to B_ν we obtain the B-field equations of motion,

$$\nabla_\mu B^{\mu\nu} - M_B^2 B^\nu = -g\bar{\psi}\underline{\gamma}^\nu\psi\,, \tag{2.9}$$

and doing so for the fermionic fields leaves us with,

$$\underline{\gamma}^\mu D_\mu \psi = im\psi\,, \quad D^*_\mu \bar{\psi}\underline{\gamma}^\mu = -im\bar{\psi}\,, \tag{2.10}$$

which are the modified Dirac equations.

Let us start by analysing the vectorial equations. We can identify on the right-hand side of the equation (2.9) the fermionic 4-current $j^\nu = -g\bar{\psi}\underline{\gamma}^\nu\psi$. After expanding the covariant derivative using the Christoffel symbols, the Proca equations in a background of B are obtained:

$$-\nabla^2 B_0 + \partial_0\partial_i B_i + a^2 M_B^2 B_0 = -a^3 g\overline{\psi}\gamma^0\psi\,, \tag{2.11}$$

$$-\partial_0^2 B_i + \nabla^2 B_i - \partial_i\partial_j B_j + \partial_0\partial_i B_0 - M_B^2 B_i a^2 = -a^3 g\overline{\psi}\gamma^i\psi\,. \tag{2.12}$$

The cosmological principle imposes that, on average, we should not expect to have net fermionic 3-currents on cosmic scales. Being consistent with this, it is assumed that the spatial components of the vectorial field are zero. The homogeneity assumption also demands that on large scales, there is no spatial dependence of the fields, leaving us with,

$$B_0 = -\frac{g\psi^\dagger\psi\, a^3}{a^2 M_B^2} \equiv \frac{\rho_c}{a^2 M_B^2}\,. \tag{2.13}$$

We have defined ρ_c, which is the commoving charge density; in the following lines, we provide more details about it. Taking the massless limit, $M_B \to 0$, may seem concerning at first glance. In appendix A, we will examine what occurs in that case and explain why we are interested in considering the non-zero mass term in a charged cosmological context.

The structure of the fermionic current also restricts the classical solutions. One can prove that j^μ is conserved by computing the derivative and substituting the EoM (2.10), as follows,

$$\nabla_\mu j^\mu = \nabla_\mu\bar{\psi}\underline{\gamma}^\mu\psi + \bar{\psi}\underline{\gamma}^\mu\nabla_\mu\psi = (-im\bar{\psi} + igB_\mu\bar{\psi}\underline{\gamma}^\mu)\psi + \bar{\psi}(im\psi - igB_\mu\underline{\gamma}^\mu\psi) = 0\,. \tag{2.14}$$

It has been used that, as explained in section 2.1, gamma matrices are defined to be covariantly constant over the manifold. Expanding the covariant derivative, it is obtained

$$\nabla_\mu j^\mu = \partial_\mu(\bar{\psi}\underline{\gamma}^\mu\psi) + \Gamma^\mu_{\nu\mu}\bar{\psi}\underline{\gamma}^\nu\psi = 0 \implies \partial_\mu(\bar{\psi}\underline{\gamma}^\mu\psi) = -\frac{4a'}{a^2}\psi^\dagger\psi\,, \tag{2.15}$$

now, taking into account that only the 0^{th} component is not zero, we can extract a condition for the charge density:

$$\partial_0(\psi^\dagger\psi) = -\frac{3a'}{a}\psi^\dagger\psi \implies \psi^\dagger\psi \propto a^{-3}\,, \tag{2.16}$$

meaning that it decays with the volume expansion. This is the reason why it was convenient to define ρ_c in (2.13) as the comoving fermionic charge density, which remains constant. The existence of a non-zero charge cannot be explained from (2.8). There must be a mechanism that unleashes the asymmetry, and the existence of such a charge will be assumed as a starting point. This will demand the consideration of an additional parameter in our model: the present value of the fermionic asymmetry Δn_f^0.

The fact that our vectorial field is massive demands one extra condition to be satisfied. It arises from taking the derivative ∇_ν of the EoM (2.9), giving

$$\nabla_\nu B^\nu = 0 \implies B^0 \propto a^{-4}\,. \tag{2.17}$$

This result is consistent with the solution found in (2.13).

2.4 Fermionic solutions in a classical background of *B*-field

We must focus now on the Dirac particles. Fermions are fundamentally quantum, and they must obey a set of anticommutation relations. This implies that there is no such thing as a classical solution for a fluid of fermions. Even so, solutions for individual fermions can be found and, from them, the quantised field can be constructed. In the following lines, we will derive them from (2.10), in the presence of the sourcing generated by the classical B^μ field. The findings in this section will provide us with the necessary technology to compute amplitudes of processes for fermions under this vectorial bath, it will consist on an essential toolkit to construct the evolution of each species population.

We start by obtaining the dispersion relations that such particles must satisfy. They can be derived by computing the modified Klein-Gordon equation, which arises from applying twice the Dirac operator on the fermion field:

$$\left[\frac{i}{a}\gamma^\alpha(\partial_\alpha - \Gamma_\alpha + igB_\alpha) - m\right]\left[\frac{i}{a}\gamma^\beta(\partial_\beta - \Gamma_\beta + igB_\beta) + m\right]\psi = 0. \tag{2.18}$$

Using the spinorial connection (2.6) we can write $\gamma^\alpha\Gamma_\alpha = -3a'/(2a)\gamma^0$. It is convenient to reformulate the last equation in terms of a new vectorial operator, $\Pi_\alpha = \frac{1}{a}(i\partial_0 + \frac{3ia'}{2a} - gB_0, i\partial_i)$, that will be contracted with the gamma matrices, and commutes with them:

$$\Big(\gamma^\alpha\Pi_\alpha - m\Big)\Big(\gamma^\beta\Pi_\beta + m\Big)\psi = \Big(\gamma^\alpha\gamma^\beta\Pi_\alpha\Pi_\beta - m^2\Big)\,\psi = 0. \tag{2.19}$$

Now we can divide the non-trivial term into two independent components,

$$\gamma^\alpha\gamma^\beta\Pi_\alpha\Pi_\beta = \gamma^\alpha\gamma^\beta\Pi_\alpha\Pi_\beta\big|_{\alpha=\beta} + \gamma^\alpha\gamma^\beta\Pi_\alpha\Pi_\beta\big|_{\alpha\neq\beta}. \tag{2.20}$$

The first one can be computed using the properties of the gamma matrices,

$$\gamma^\alpha\gamma^\beta\Pi_\alpha\Pi_\beta\big|_{\alpha=\beta} = \left(\gamma^0\right)^2(\Pi_0)^2 + \left(\gamma^i\right)^2(\Pi_i)^2 = (\Pi_0)^2 - \sum_i(\Pi_i)^2. \tag{2.21}$$

The second can be expanded as,

$$\gamma^\alpha\gamma^\beta\Pi_\alpha\Pi_\beta\big|_{\alpha\neq\beta} = \frac{1}{2}\Big(\gamma^\alpha\gamma^\beta\Pi_\alpha\Pi_\beta + \gamma^\beta\gamma^\alpha\Pi_\beta\Pi_\alpha\Big)\big|_{\alpha\neq\beta}\,, \tag{2.22}$$

and now using that for $\alpha\neq\beta$ we have $\gamma^\alpha\gamma^\beta = -\gamma^\beta\gamma^\alpha$,

$$\begin{aligned} &= \frac{1}{4}\Big(\gamma^\alpha\gamma^\beta\Pi_\alpha\Pi_\beta - \gamma^\beta\gamma^\alpha\Pi_\alpha\Pi_\beta + \gamma^\beta\gamma^\alpha\Pi_\beta\Pi_\alpha - \gamma^\alpha\gamma^\beta\Pi_\beta\Pi_\alpha\Big)\big|_{\alpha\neq\beta} \\ &= \frac{1}{4}[\gamma^\alpha,\gamma^\beta][\Pi_\alpha,\Pi_\beta]\big|_{\alpha\neq\beta}\,. \end{aligned} \tag{2.23}$$

It is important to remember that the solution we consider takes the form $B_0 = B_0(\eta)$, which implies for the commutator $[\Pi_\alpha, \Pi_\beta] = 0$ for $\alpha \neq \beta$. Only the $\alpha = \beta$ terms of equation (2.19) contribute, and we can write

$$\left[(\Pi_0)^2 - \sum_i (\Pi_i)^2\right]\psi = 0\,. \tag{2.24}$$

After expanding the Π_μ operators acting on ψ, we find,

$$\begin{aligned}\Bigg[-\partial_0^2 + \nabla^2 - \left(2\frac{a'}{a} + 2igB_0\right)\partial_0 - \frac{3}{2}\frac{a''}{a} + \frac{3}{4}\left(\frac{a'}{a}\right)^2 \\ -2igB_0\frac{a'}{a} - ig(\partial_0 B_0) + g^2 B_0^2 - a^2 m^2\Bigg]\psi = 0\,.\end{aligned} \tag{2.25}$$

This result is far from trivial; there was no guarantee that the Klein-Gordon equation would be diagonal, given the specific structure of the sourcing term of B. The typical frequencies of oscillation of particles, which are proportional to their momentum, are orders of magnitude above the Hubble rate at conventional cosmological epochs, i.e. for temperatures below chiral symmetry recovery. Having this into acount we can neglect terms proportional to the Hubble rate in front of others,

$$\left[-\partial_0^2 + \nabla^2 - 2igB_0\partial_0 + g^2B_0^2 - a^2m^2\right]\psi = 0\,. \tag{2.26}$$

It is convenient to perform a change of coordinates $x^\mu \to x^\mu/a$, $B_\mu \to B_\mu/a$, which will be adopted from now on. Under this change, the metric becomes the Minkowski space one, and

$$\left[-\partial_0^2 + \nabla^2 - 2igB_0\partial_0 + g^2B_0^2 - m^2\right]\psi = 0\,. \tag{2.27}$$

Taking guidance from the Minkowskian case, we propose a plane wave independent solutions $\psi_\pm = f_s(p)e^{\pm ipx}$, which yield the dispersion relations

$$(E_\pm \pm gB^0)^2 = |\vec{p}|^2 + m^2\,. \tag{2.28}$$

The spinorial structure can be obtained by solving the modified Dirac equation. After neglecting the terms that contain the Hubble rate in (2.10), we have,

$$\left[\gamma^\mu(i\partial_\mu - gB_\mu) + m\right]\psi = 0 \tag{2.29}$$

Let's discuss $\psi_\pm$ cases individually. For $\psi_+ = u_s(p)e^{ipx}$ we have,

$$\left[\gamma^\mu(p_\mu + gB_\mu) - m\right]u_s(\vec{p}) = 0\,. \tag{2.30}$$

We must remember that the 4-momentum of these particles is given by $p^\mu = (E_+, \vec{p})$. Now defining $u_s(\vec{p}) = (\varphi,\, \chi)^T$ and $\pm E_M = E_+ + gB^0 = \sqrt{|\vec{p}|^2 + m^2}$ we can rewrite our equation as,

$$\begin{pmatrix} \mp E_M & \vec{p}\cdot\vec{\sigma} \\ -\vec{p}\cdot\vec{\sigma} & \pm E_M \end{pmatrix}\begin{pmatrix}\varphi \\ \chi\end{pmatrix} = m\begin{pmatrix}\varphi \\ \chi\end{pmatrix} \tag{2.31}$$

Noticing that $(\vec{p}\cdot\vec{\sigma})^2 = |\vec{p}|^2 = (E_+ + gB^0)^2 - m^2 = (E_M + m)(E_M - m)$ we can write the solution of this system of equations for both cases $\pm E_M$ as follows:

$$u_{s+}(\vec{p}) = \sqrt{E_M + m}\begin{pmatrix} \frac{(\vec{p}\cdot\vec{\sigma})}{E_M+m}\chi_s \\ \chi_s \end{pmatrix}, \quad u_{s-}(\vec{p}) = \sqrt{E_M + m}\begin{pmatrix} \varphi_s \\ \frac{-(\vec{p}\cdot\vec{\sigma})}{E_M+m}\varphi_s \end{pmatrix}. \tag{2.32}$$

We are left with the freedom to choose a basis for the two spinors χ and φ, which we determine to be two linearly independent states for each, normalized as $\chi_s^\dagger\chi_{s'} = \varphi_s^\dagger\varphi_{s'} = \delta_{ss'}$.

Let's proceed analogously for ψ_-, in momentum space we have

$$\left[\gamma^\mu(p_\mu - gB_\mu) + m\right] v_s(\vec{p}) = 0\,, \tag{2.33}$$

with $p^\mu = (E_-, \vec{p})$, $v_s(\vec{p}) = (\varphi, \chi)^T$ and $\pm E_M = E_- - gB^0 = \sqrt{|\vec{p}|^2 + m^2}$. Expanding in matrix form,

$$\begin{pmatrix} \pm E_M & -\vec{p}\cdot\vec{\sigma} \\ \vec{p}\cdot\vec{\sigma} & \mp E_M \end{pmatrix}\begin{pmatrix} \varphi \\ \chi \end{pmatrix} = m\begin{pmatrix} \varphi \\ \chi \end{pmatrix} \tag{2.34}$$

we obtain the solutions:

$$v_{s+}(\vec{p}) = \sqrt{E_M + m}\begin{pmatrix} \varphi_s \\ \frac{(\vec{p}\cdot\vec{\sigma})}{E_M+m}\varphi_s \end{pmatrix}, \quad v_{s-}(\vec{p}) = \sqrt{E_M + m}\begin{pmatrix} \frac{-(\vec{p}\cdot\vec{\sigma})}{E_M+m}\chi_s \\ \chi_s \end{pmatrix}, \tag{2.35}$$

and similar normalisations. The general solution for the field can be constructed in terms of the 4 apparently linearly independent solutions,

$$\begin{aligned}\psi = \int \frac{d^3\vec{p}}{(2\pi)^3}\frac{1}{\sqrt{2E_M}}\sum_s \Big[&A(\vec{p})e^{ip_+x}u_{s+}(\vec{p}) + B(\vec{p})e^{ip_-x}u_{s-}(\vec{p}) \\ &+C(\vec{p})e^{-ip_+x}v_{s+}(\vec{p}) + D(\vec{p})e^{-ip_-x}v_{s-}(\vec{p})\Big]\,,\end{aligned} \tag{2.36}$$

where the energy prefactor is common for all terms and comes from demanding on-shell condition for the four kind of solutions and integrating out on p^0. For example, for u-type solutions we have:

$$\begin{aligned}&\int \frac{d^4p}{(2\pi)^4}(2\pi)\,\delta\left((p^0 + gB^0)^2 - |\vec{p}|^2 - m^2\right) \\ &= \int \frac{d^4p}{(2\pi)^3}\frac{\delta(p^0 - E_+)}{2(E_+ + gB^0)} = \int \frac{d^3\vec{p}}{(2\pi)^3}\frac{1}{2E_M}\,.\end{aligned} \tag{2.37}$$

Nevertheless, the solutions above are not completely independent,

$$u_s(\vec{p}) \equiv u_{s+}(\vec{p}) = v_{s-}(-\vec{p})\,, \quad v_s(\vec{p}) \equiv v_{s+}(\vec{p}) = u_{s-}(-\vec{p})\,. \tag{2.38}$$

Thus, by sending $\vec{p} \to -\vec{p}$ for the second and fourth terms, and working out each power of the exponentials we reduce the field to the following expression,

$$\psi(x) = e^{igB^0x^0}\int \frac{d^3\vec{p}}{(2\pi)^3}\frac{1}{\sqrt{2E_M}}\sum_s \left[e^{ip_Mx}u_s(\vec{p})a_s(\vec{p}) + e^{-ip_Mx}v_s(\vec{p})b_s^\dagger(\vec{p})\right], \tag{2.39}$$

where $p_M \equiv (E_M, \vec{p})$ and $a_s(\vec{p})$ and $b_s^\dagger(\vec{p})$ are the usual particle and antiparticle annihilation and creation operators that satisfy the anticommutation relations. From (2.39) it stands out that the interaction does not affect the fermionic propagator because the combination $\bar{\psi}(x)\psi(x')$ makes global phases vanish in the limit of instantaneous point-like interactions.

The normalization properties of the spinors are:

$$\begin{aligned} \bar{u}_s(\vec{p})u_{s'}(\vec{p}) = -2m\delta_{ss'}\,, \quad \bar{u}_s(\vec{p})v_{s'}(\vec{p}) = 0\,, \quad \bar{v}_s(\vec{p})v_{s'}(\vec{p}) = 2m\delta_{ss'} \\ u_s^\dagger(\vec{p})u_{s'}(\vec{p}) = 2E_M\delta_{ss'}\,, \quad v_s^\dagger(\vec{p})v_{s'}(\vec{p}) = 2E_M\delta_{ss'}\,, \end{aligned} \tag{2.40}$$

and, the completeness relations

$$\sum_s u_s(\vec{p})\bar{u}_s(\vec{p}) = -\left[\gamma^\mu(p_\mu - gB_\mu) + m\right], \tag{2.41}$$

remember, with $p^\mu = (E_+, \vec{p})$; and

$$\sum_s v_s(\vec{p})\bar{v}_s(\vec{p}) = -\left[\gamma^\mu(p_\mu + gB_\mu) - m\right], \tag{2.42}$$

with $p^\mu = (E_-, \vec{p})$. These results are indispensable for the computation of Feynman diagrams and will be employed subsequently.

2.5 Stress-energy tensors: energy density and pressure

Each particle species contributes to the cosmological background through its pressure and energy density. The dependence arises naturally from Einstein's equations, obtained by extremizing the total action, including the Einstein-Hilbert term, with respect to the metric tensor,

$$R_{\mu\nu} - \frac{1}{2}Rg_{\mu\nu} = 8\pi G T_{\mu\nu}\,. \tag{2.43}$$

The stress-energy tensor (SET) in the right-hand side of the equation consists of the sourcing of all matter fields to gravitation. This section analyses the energy-momentum tensor components associated with fermions and the B field, incorporating their interaction term. The pure bosonic SET, excluding the interaction term, is given by,

$$\begin{aligned} T^B_{\mu\nu} &= -2\frac{\partial\mathcal{L}_B}{\partial g^{\mu\nu}} + g_{\mu\nu}\mathcal{L}_B = \\ &= g^{\alpha\beta}B_{\alpha\mu}B_{\beta\nu} + M_B^2 B_\mu B_\nu + g_{\mu\nu}\left[-\frac{1}{4}B_{\alpha\beta}B^{\alpha\beta} - \frac{1}{2}M_B^2 B_\alpha B^\alpha\right], \end{aligned} \tag{2.44}$$

where $\mathcal{L}_B$ is the Lagrangian density of the B field. Imposing the symmetries of the classical solutions of the B field, the following non-zero components are found:

$$T^B_{00} = \frac{1}{2}M_B^2 B_0^2\,, \quad T^B_{ij} = \frac{1}{2}M_B^2 B_0^2 \delta_{ij}\,. \tag{2.45}$$

From them the energy density and pressure are derived,

$$\rho_B^{\text{clas.}} = P_B^{\text{clas.}} = \frac{\rho_c^2}{2M_B^2 a^6}\,. \tag{2.46}$$

This solution describes a perfect fluid characterised by the equation of state

$$\omega_B \equiv P_B^{\text{clas.}} / \rho_B^{\text{clas.}} = 1\,, \tag{2.47}$$

which is conventionally termed kination in the literature [10]. This rapidly decaying component can dominate cosmology for a specific combination of mass, coupling, and commoving fermionic charge during some periods. In the following sections, various scenarios are explored, including this case.

Obtaining the fermionic SET is not as simple as for the B field. The Dirac component of the action depends non-trivially on the metric through the tetrad; therefore, obtaining the fermionic SET requires a more involved approach [11]. The full-fledged tensor is given by

$$T^f_{\mu\nu} = \frac{i}{2}\left[\bar{\psi}\underline{\gamma}_{(\mu}D_{\nu)} - D^*_{(\mu}\bar{\psi}\underline{\gamma}_{\nu)}\psi\right] + \frac{i}{2}g_{\mu\nu}\left[\bar{\psi}\underline{\gamma}^\alpha D_\alpha\psi - D^*_\alpha\bar{\psi}\underline{\gamma}^\alpha\psi\right] - m\bar{\psi}\psi g_{\mu\nu}\,, \tag{2.48}$$

where the symmetrisation of indices is defined as,

$$A_{(a}B_{b)} = \frac{1}{2}\left(A_a B_b + A_b B_a\right)\,. \tag{2.49}$$

For on-shell fermions we can use the EoM and simplify the expression,

$$T^f_{\mu\nu} = \frac{i}{2}\left[\bar{\psi}\underline{\gamma}_{(\mu}D_{\nu)}\psi - D^*_{(\mu}\bar{\psi}\underline{\gamma}_{\nu)}\psi\right]\,. \tag{2.50}$$

After expanding the derivatives, one obtains the following components:

$$T^f_{00} = a^2\left[m\bar{\psi}\psi - \frac{i}{2}(\partial_i\bar{\psi}\underline{\gamma}^i\psi - \bar{\psi}\underline{\gamma}^i\partial_i\psi)\right]\,, \quad T^f_{ij} = \frac{i}{2}\left[\bar{\psi}\underline{\gamma}_{(i}\partial_{j)}\psi - \partial_{(j}\bar{\psi}\underline{\gamma}_{i)}\psi\right]. \tag{2.51}$$

These expressions show the expected behaviour of a cosmological fermionic fluid in two basic scenarios. For non-relativistic fermions, the terms that contain derivatives of the Dirac field are proportional to their momentum and are negligible in front of the rest mass. In this limit, it is obtained $\omega_f = 0$, which corresponds to the equation of state parameter of non-relativistic matter. On the other hand, for high energies, the mass term is negligible and it is recovered the radiation equation of state parameter, $\omega_f = 1/3$. Building on these results, we are compelled to consider the contribution of the fermions under the interaction of the Bs by constructing the particle and antiparticle distribution functions, f_f and $f_{\bar{f}}$, respectively. This can be implemented by getting track of the changes on the shape and temperature due to interactions of both fields, which potentially shift the distributions away from the equilibrium ones. If the distributions are known, the number density, energy density and pressure of the fluid can be obtained using the standard definitions:

$$n = \frac{\mathfrak{g}}{(2\pi)^3}\int d^3\vec{p}\, f(\eta,\vec{p})\,, \tag{2.52}$$

$$\rho = \frac{\mathfrak{g}}{(2\pi)^3}\int d^3\vec{p}\sqrt{|\vec{p}|^2 + m^2}\, f(\eta,\vec{p})\,, \tag{2.53}$$

$$P = \frac{\mathfrak{g}}{(2\pi)^3}\int d^3\vec{p}\frac{|\vec{p}|}{3\sqrt{|\vec{p}|^2 + m^2}}\, f(\eta,\vec{p})\,. \tag{2.54}$$

These expressions apply to both bosons and fermions, and for the second ones even in the presence of the background of Bs. This arises because the background term in the fermion's total energy—specifically, the $\pm gB^0$ contribution in $E_\pm = \sqrt{|\vec{p}|^2 + m^2} \pm gB^0$—acts as a potential energy. This term has already been incorporated into the classical energy density component in (2.46).

A particle species in thermal equilibrium follows the distribution

$$f(\eta, \vec{p}) = \frac{1}{\exp\left(\frac{E(\vec{p})-\mu}{T}\right) \pm 1}, \tag{2.55}$$

with $+$ corresponding to fermions and $-$ to bosons, E is the energy, μ the chemical potential and T the temperature of the fluid of particles in consideration. We will assume that the fermions were in the past in thermal equilibrium, and that they decouple from the radiation fluid while being relativistic, i.e. $E = |\vec{p}|$. After the decoupling, the shape of the distribution will not be affected, unless the interactions with the Bs become relevant. The net asymmetry of a relativistic fermion species that annihilates efficiently into uncharged vectors compared with the rate of expansion of the universe is given by [12]:

$$n_f - n_{\bar{f}} = \frac{\mathfrak{g}_f T^3}{6\pi^2}\left[\pi^2 \frac{\mu}{T} + \left(\frac{\mu}{T}\right)^3\right] \tag{2.56}$$

where $\mu \equiv \mu_f = -\mu_{\bar{f}}$. This is also the case for species that are relativistic at the moment at which they leave thermal equilibrium with the radiation fluid, and continue to apply after they become non-relativistic. The chemical potential will evolve with temperature, as dictated by equation (2.56) and the dilution law $n_f - n_{\bar{f}} \propto \psi^\dagger\psi \propto a^{-3}$. The evolution will therefore depend on the parameters g and Δn_f^0.

During radiation domination, temperature will dilute as $T \propto a^{-1}$ and will be shared by all species in thermal equilibrium. When a species is decoupled, its temperature becomes independent from that of the radiation fluid and its number density decays as $n \propto a^{-3}$. In the following sections, we will explain possible contributions to the evolution of the temperature of thermal fluids.

In addition to the classical component of B field, it is considered the fluid of its particles. The contribution is thermal and can be computed by keeping track of the occupation of the energy levels, following the boson distribution function as explained for fermions.

2.6 Computing rates, finding the dominant scattering processes in cosmic evolution

As pointed out when the model was introduced in section 2.2, we aim to obtain the evolution of the particle populations of our model. Certain cosmological epochs permit simpler calculations of this than others. For relativistic bosonic species in thermal equilibrium expressions (2.53) and (2.54) simplify to

$$\rho_b = \frac{\pi^2}{30} g_b T^4, \quad P_b = \rho_b/3. \tag{2.57}$$

There are analogous expressions for a fermionic fluid,

$$\rho_f = \frac{7}{8}\frac{\pi^2}{30} g_f T^4 \,, \quad P_f = \rho_f/3 \,. \tag{2.58}$$

These are also true for species which are non-relativistic but decoupled from radiation being so. We can define a total relativistic energy density for all the species in equilibrium with radiation as:

$$\rho_r = \frac{\pi^2}{30} g_\star(T) T^4 \,, \tag{2.59}$$

with T the temperature of the fluid, and $g_\star(T)$ is the internal degrees of freedom of the fluid at a given temperature, given by,

$$g_\star(T) = \sum_{i\,=\,\text{bosons}} \mathfrak{g}_i \left(\frac{T_i}{T}\right)^4 + \frac{7}{8} \sum_{i\,=\,\text{fermions}} \mathfrak{g}_i \left(\frac{T_i}{T}\right)^4 . \tag{2.60}$$

The temperature dependence is tracking which species remains in equilibrium with the photons. We may specify what *thermal equilibrium* means in this context. We say that some species reach equilibrium if the rate of interactions is high enough for the fluid to maintain a balanced, uniform, thermal state. We assume that, early enough, all species will be in this situation. The continuous scatterings of the fluid's particles allow it to maintain equilibrium, sharing a common temperature. These interactions effectively counteract the expansion of the universe, which, if it dominates, would prevent achieving the thermal state. When the rate of interactions is not sufficient, we say that the species decouples from the radiation fluid that keeps being in equilibrium. After its decoupling, the energy density of the considered particles dilutes away, as explained in section 2.2, depending on whether the species is relativistic or not. Another important effect to take into account is the decay. After becoming unstable and decaying, the population of particles gets reduced at the cost of increasing the number density of generated particles from another species. This implies that exists an energy injection from the initial fluid into the second one, affecting its properties.

Our approach will be to identify the specific epochs in each species' cosmological evolution where its interaction rate dominates over the Hubble rate, and vice versa. By doing so, we will map out the distinct regimes and physical phenomena described earlier, enabling us to predict the behaviour and properties of each population. The first considered rate is that of producing Bs from the annihilation of a fermion-antifermion pair. It is given by:

$$\Gamma_{f\bar{f}\to B} \simeq \left(M_B^2 + s^2\right)^{-3/2} \langle \sigma v_{\text{rel}} \rangle \, n_f n_{\bar{f}} \,. \tag{2.61}$$

Details on the calculation of this and other rates can be found in appendix B. This process corresponds to a peak of production when temperatures are of the order of the mass of the produced particle, and tends to dominate only in this condition. It is therefore necessary to take into account processes that include two vertices of interaction, such as $fB \leftrightarrow fB$. Their rate is effectively given by,

$$\Gamma_{fB\leftrightarrow fB} \simeq \begin{cases} g^4 \left(\frac{T^2}{M^4} + \frac{1}{T^2}\right) n_f v_{\text{rel.}} & \text{if } T < T_{\text{chiral}} \,, \\ g^4 \left(\frac{1}{T^2}\right) n_f v_{\text{rel.}} & \text{if } T > T_{\text{chiral}} \end{cases} \,, \tag{2.62}$$

which includes the longitudinal (weak force-like) and transverse modes (Compton-like) in case the B is massive, and only the transverse otherwise. Finally, the decay rate allows us to point out the moment at which the particle becomes unstable, and it is given by:

$$\Gamma_{B\to f\bar{f}} = \frac{g^2 M_B}{48\pi}\left(1+\frac{2m^2}{M_B^2}\right)\sqrt{1-\frac{4m^2}{M_B^2}}\,. \tag{2.63}$$

The rate of expansion of the universe will be computed with the Hubble rate in the ΛCDM with standard parameters [2]. In principle, for temperatures higher than the e^-e^+ annihilation, it would be necessary to use the thermal components of the energy density instead of the classical dilution of matter and radiation. Even so, the thermal contribution from the vector is negligible in front of the other degrees of freedom at high temperatures. Moreover, it is more convenient to use the usual dilution laws at late times.

Each process will compete effectively if $\Gamma_i \sim H$, and dominate if the first surpasses the Hubble. In general, there will be situations in which different processes will contribute comparably, and we will not be able to predict which is the resulting particle distributions. These regimes are out of our analysis, and may be computed using the so-called Boltzmann equations. This integrodifferential system allows for solving the distribution of particles in a general scenario. There is a corresponding equation of the following form for each particle species,

$$\frac{dn_i}{dt} + 3Hn_i = \frac{\mathfrak{g}_i}{(2\pi)^3}\int C[f_i]\frac{d^3p}{E}\,. \tag{2.64}$$

It accounts for the competition between the background evolution, given by the Hubble rate, and the microphysical processes included in the right-hand side through the collision term $C[f_i]$. While this represents the general approach for studying any scenario, our proposal enables exploration of the parameter space in an intuitive, straightforward, and computationally efficient manner. In the following section, the resulting analysis of the parameter space will be displayed. After that, three different scenarios are explored in which non-trivial effects arise in cosmological observables.

3 Phenomenology. Three scenarios [1]

We focus now in the case in which the generic fermion corresponds to neutrinos. As a first approach to study the phenomenology of this system, we choose $\Delta n_f^0 = 10^{-9} n_\nu^0$, motivated by the present baryon asymmetry. A key advantage of the model for future implementation of cosmological fits will be its ability to set an upper limit for this parameter, which is currently challenging to determine experimentally. The current number density of neutrinos, as well as the sum of the masses of the families, are much more constrained observables [13]. The mass of the neutrinos is taken to be the upper limit of the sum of the masses, $m \simeq 0.1\,\mathrm{eV}$. For this value of the asymmetry parameter, the classical solutions of the B field become strongly suppressed, and their contribution to the energy density and pressure is negligible in front of the thermal components. This is so, even if $\rho_B^{\mathrm{cl.}} \propto a^{-6}$, because this

[1]The source code is accessible at: https://github.com/amunozna/fermion-vector-cosmo-coupling.git

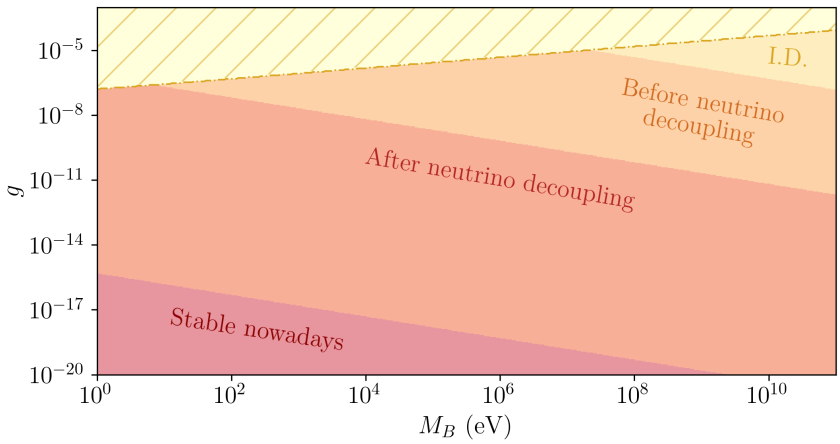

Figure 2. Moment at which the decay of B particles is the dominating process, over the parameter space of our interaction model: g is the coupling between fermions and vectors and M_B the mass of the Proca-like field. The fermionic asymmetry is fixed to $\Delta n_f^0 = 10^{-9} n_\nu^0$. I.D. stands for instantaneous decay; the particle is unstable from the moment it gets mass, meaning that the fluid of Bs has not been in thermal equilibrium while massive. The dashed region corresponds to regimes where production and decay rates are comparable during a significant portion of the cosmological evolution; solving the Boltzmann equation is necessary for these pairs of parameters to determine where the decay is the dominating contribution.

solution is only valid for temperatures below the symmetry-breaking scale. Evolving $\rho_B^{\text{cl.}}$ from the present, $a_0 = 1$, until the breaking scale, $a(T_{\text{chiral}})$, it is seen that this term is negligible. This is the case of the two scenarios that will be presented in the next pages. The third scenario of this section corresponds to an opposite situation: the main contribution is classical at early times. For the moment, we will focus on the case of the dominating thermal component.

Shortly after Γ_B becomes larger than the other rates, equation (2.64) gives an exponentially decaying solution for n_B. This implies that all the B particle content decays to neutrino-antineutrino pairs. Studying at which temperature this situation happens, depending on the value of g and M_B, we can characterise different regions of our parameter space. The result of this analysis is displayed in figure 2. In situations in which $\Gamma_{f\bar{f}\to B}$ or the 2 to 2 particle rates compete with the decay rate of the B during a significant fraction of the cosmological evolution we cannot predict the population without solving the Boltzmann equation; these cases are outside our range of study. It also exists the possibility that the decay rate Γ_B dominates even in the epoch at which the vectors acquire mass. In that case, which will be referred to as I.D. (instantaneously decaying), the vectors decay immediately after becoming massive. This implies that the fluid hasn't survived long enough to be in thermal equilibrium while massive. In the following, we explain the implications on cosmological observables of the early and the late decay of the Bs.

3.1 Decay before the neutrino decoupling

The following procedure is performed by opting for the particular selection $g = 10^{-7}$, $M_B = 10^5\,\text{eV}$; but reproduces the expected physical effects of the corresponding region in

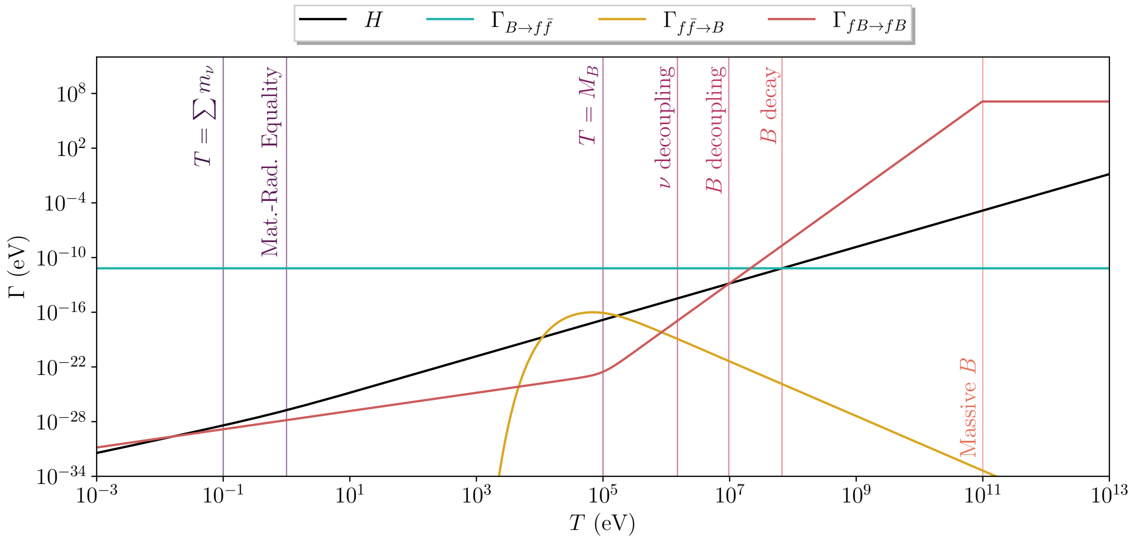

Figure 3. Evolution of rates of scatterings and expansion rate, given by the Hubble parameter, as a function of the temperature of the photon fluid. This particular selection of parameters corresponds to a vector field that decays into neutrinos before they decouple from the radiation fluid, $\Delta n_f^0 = 10^{-9} n_\nu^0$, $g = 10^{-7}$, $M_B = 10^5\,\text{eV}$.

figure 2. The result of the evolution of the rates is displayed in figure 3.

At temperatures higher than the symmetry-breaking scale, the vector is massless and the decay rate of 2 to 2 interactions is proportional to the temperature, as usual for processes with massless particles involved. This is obtained from equation (2.62), noticing that in this regime fermions are in equilibrium and relativistic, $n_f \propto T^3$. The distribution f_B corresponds to the equilibrium one, as the scatterings are frequent. After they gain mass, the temperature dependence intensifies as $\Gamma \propto T^5$ and the rate falls, but the species remain in equilibrium with radiation. When the decay rate Γ_B crosses the Hubble, the decaying process becomes efficient and starts competing with the 2 to 2. It would be necessary to solve the Boltzmann equations to know the distribution functions at this epoch; all terms are of the same order and competing. After the Hubble surpasses the 2 to 2 rates, interactions are not happening frequently enough, implying that B decouples from neutrinos and, thus, from the radiation fluid. At the last stages between the moment at which the particle becomes unstable and the decoupling, the number density of Bs will start lowering, and not much later, we will not keep any of them.

During the decay, all the energy of these particles is transferred to the neutrino fluid by heating its temperature. Neutrinos are still coupled to the relativistic fluid particles and thus share temperature with them. The temperature rise can be computed by imposing:

$$\rho_r|_{\text{after}} = \rho_r|_{\text{before}} + \rho_B|_{\text{before}}\,, \tag{3.1}$$

where *before* and *after* refer to before and after the decay of the particle, respectively, and ρ_r is the energy density of the relativistic fluid. For this fluid in thermal equilibrium, we must use the expression (2.59). Solving for the temperature at the instant after the decay,

$$T|_{\text{after}} = \left(T|_{\text{before}}^4 + \frac{\rho_B|_{\text{before}}}{(\pi^2/30)g_\star(T|_{\text{before}})} \right)^{1/4}, \tag{3.2}$$

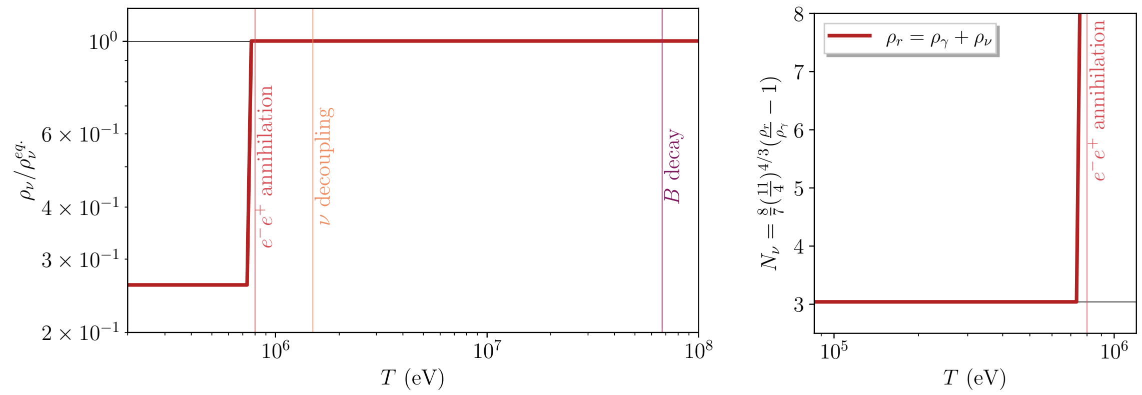

Figure 4. Effects on cosmological observables in the case of the B decaying before the neutrino decoupling. Left: rate between the energy density of the fluid of neutrinos and the energy density it would have in case they remained coupled with photons during all cosmological evolution as a function of the temperature of the photon, T. These energy densities contain both particle and antiparticle contributions. Right: effective number of neutrino species as a function of T.

and for temperatures from that moment onward, we can use $\tilde{T} = (T|_{\text{after}}/T|_{\text{before}})T$ to account for the energy injection in the fluid. After the temperature lowers, at $\tilde{T} \sim 1.5\,\text{MeV}$, neutrinos decouple and evolve with an independent temperature; their comoving entropy density is conserved individually. A little later, at $\tilde{T} \sim 0.8\,\text{MeV}$, electron and positron pairs annihilate, heating the remaining photon fluid, but not the neutrino one. The effect of this temperature rise of the photons with respect to the neutrinos can be observed in the left graph of figure 4, where the neutrino energy density is lower than it would have been in equilibrium after the annihilation. This rise in the temperature can be computed taking into account that the entropy per commoving volume, which is shared between fluids in equilibrium, is conserved due to the second law of thermodynamics. The temperature rise is given by comparing the internal degrees of freedom before and after the annihilation and demanding that the entropy is conserved, obtaining $\tilde{T}_\gamma = (\frac{11}{4})^{1/3}\tilde{T}_\nu$.

We want to emphasise that in this situation, there is no imprint left on the effective number of neutrinos N_ν, since the energy injection from the B's decay was common to all relativistic particles before neutrino decoupling. This is reflected in the right graph of the figure 4. This number is defined as [13]

$$N_\nu = \frac{8}{7}\left(\frac{11}{4}\right)^{4/3}\left(\frac{\rho_r}{\rho_\gamma} - 1\right) , \tag{3.3}$$

and counts the number of relativistic species, apart from the photons, after the e^+e^- annihilation. The cosmological observable that is imprinted in this situation is the population of particles produced in BBN, because the temperature of photons was affected by the energy injection of the decay.

Continuing with the evolution of the rates, when the temperature is of the order of magnitude of M_B, the production of Bs from the annihilation of neutrinos and antineutrinos becomes effective. Even that, the rate of decay is enhanced by many orders of magnitude, keeping the massive vector field unpopulated.

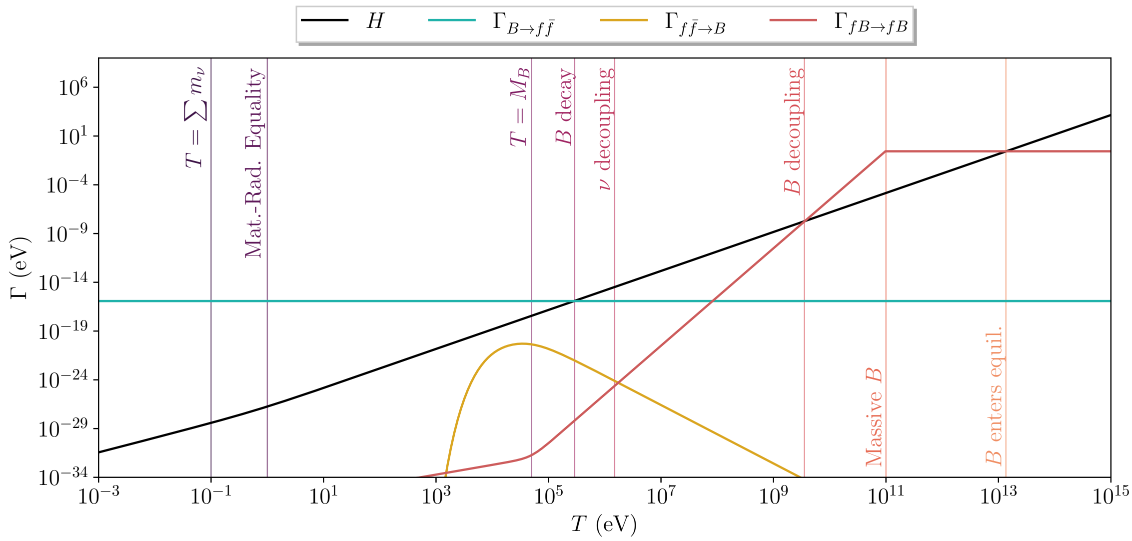

Figure 5. Evolution of rates of scatterings and expansion rate, given by the Hubble parameter, as a function of the temperature of the photon fluid. This particular selection of parameters corresponds to a vector field that decays into neutrinos after they decouple from the radiation fluid, $\Delta n_f^0 = 10^{-9} n_\nu^0$, $g = 6 \cdot 10^{-10}$, $M_B = 5 \cdot 10^4$ eV.

3.2 Decay after neutrino decoupling

Following the steps of the previous scenario, the base parameters for this discussion are $g = 6 \cdot 10^{-10}$ and $M_B = 5 \cdot 10^4$ eV. The evolution of the rates is displayed in figure 5. Differences with respect to the last case arise at the decoupling of the B; without solving the evolution via the Boltzmann equation it can be ensured that at $T \sim 10^9$ eV the vectors are completely decoupled from the radiation fluid and evolve freely until their decay. Before that happens neutrinos also decouple and the electron-positron pairs annihilate. This means that the injection of energy from the decay of the Bs affects only to neutrinos, which at the same time are outside its equilibrium distribution as they decoupled previously.

Figure 6 left displays the rate between the neutrino energy density and the one that it would have in case they shared temperature with photons. The interpretation is consistent after the decoupling, they leave equilibrium and it is evidenced after the annihilation. Following the evolution, the decay of the massive vectors makes the temperature of neutrinos rise again, reducing the difference with the equilibrium distribution. The change in temperature, that this time does not affect the photon fluid, is given by:

$$T_\nu|_{\text{after}} = \left(T_\nu|^4_{\text{before}} + \frac{\rho_B|_{\text{before}}}{\frac{7}{8}(\pi^2/30) g_\nu} \right)^{1/4} . \tag{3.4}$$

This time, N_ν is affected because the injection of energy that comes from the decay of the B is not common to all relativistic species. The effect can be seen in the right plot of figure 6, where there is an increase in the effective number of neutrinos. Therefore, including the coupling in a cosmological analysis will place a tight bound on this region of the parameter space.

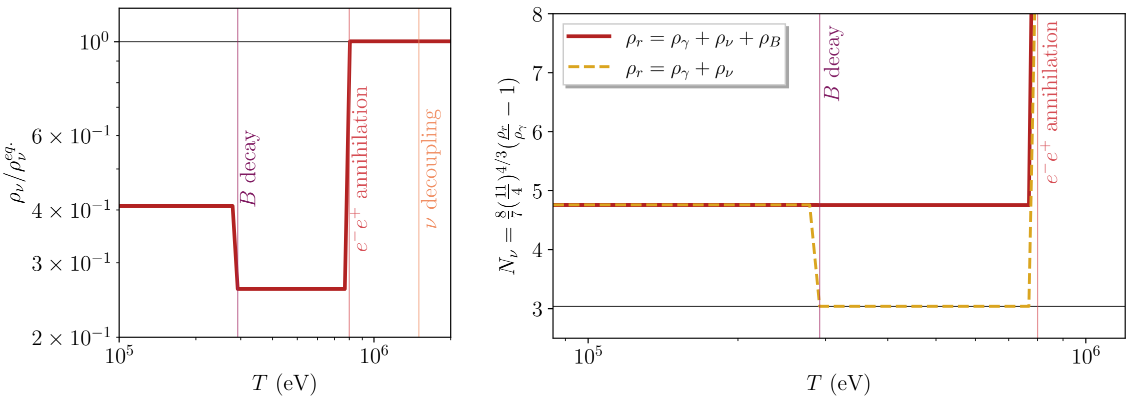

Figure 6. Effects on cosmological observables in the case of the B decaying after the neutrino decoupling. Left: rate between the energy density of the fluid of neutrinos and the energy density it would have in case they remained coupled with photons during all cosmological evolution as a function of the temperature of the photon, T. These energy densities contain both particle and antiparticle contributions. Right: effective number of neutrino species as a function of T. The continuous curve takes into account all relativistic species, the dashed only photons and neutrinos; all the energy density from the Bs is injected in the neutrino fluid after its decay.

3.3 Classical B-background leading the universe evolution

The last case that we present is a scenario in which the contribution of the classical solutions of the vectorial field dominate the energy density of the universe. Given the strong decaying behaviour, see (2.46), this is only possible during a given period of time after the vector gets mass. Additionally, this component is highly supressed by the coupling parameter g and the fermion-antifermion assymetry, both squared. On the other hand, the density is enhanced by small mass values of the vector, and this is the scenario that we will explore. Relaxing the value on the fermion-antifermion asymmetry $\Delta n_f^0 = 10^{-3} n_\nu^0$, and lowering the mass of the vector boson to $M_B = 10^{-2}\,\mathrm{eV}$ we can observe a significant contribution to the total energy density and pressure. The result is ilustrated in figure 7, where the equation of state parameter evolves non-trivially from a kination-dominated regime to the usual radiation epoch. This change on the equation of state would imprint the Hubble rate and the temperature of the radiation fluid, and thus this scenario can be constrained trough them. This contribution of energy will not be injected to any other component, it only dilutes away with the expansion of the universe.

4 Conclusions and future directions

We have proposed a model to study non-standard interactions between fermions and a massive vector particle. Starting from first principles has allowed us to obtain information about both macro and micro physics that play a precise role in the construction of the model.

Classical solutions for the vectorial field that are compatible with the CP have been obtained. These classical fields act as a background source for the fermions, whose equations of motion undergo modifications. The quantised solution of these equations has been found, as well as the modified completeness relations. All this structure permitted us to

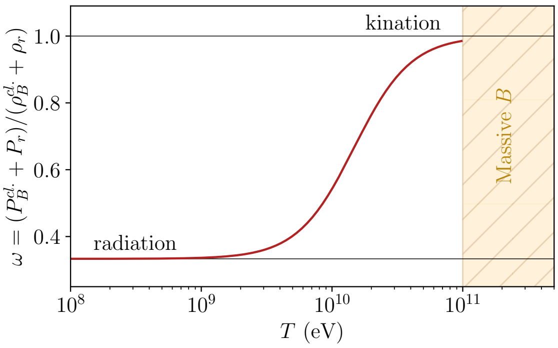

Figure 7. The total equation-of-state parameter ω for the cosmological fluid, including contributions from both radiation and the background B-field, as a function of temperature T. Black lines pinpoint the values for radiation and kination domination scenarios. The massless region is hatched as the behaviour of this parameter would depend on the mechanism in charge of providing the mass.

compute scattering amplitudes, and from them extract rates of production, interaction and decay. By chasing the competition between these processes and the expansion of the Universe, the parameter space of the theory has been characterised.

The contribution to the energy density and pressure from the classical solutions of the B field has been determined, discovering that it entails a kination equation of state. When the asymmetry between particle and antiparticle number density of the fermionic family is large and the mass of the vector boson is small, a relevant contribution of such classic solutions is possible. At early times, at the temperature scale at which the vector becomes massive, the total energy density can be dominated by $\rho_B^{\text{cl.}}$ and $\omega \simeq 1$. This implies that during a period of time, the universe will be dominated by kination instead of radiation, and the Hubble parameter will be imprinted.

Focusing on the neutrino case, their thermal energy and number density have been obtained by solving the evolution of the distribution functions of each species with the rate technology. In particular, we have concluded that in case the vector particle becomes unstable before the neutrino decoupling, the main effect on observables is through affecting the rates of production in BBN. In case that the decay occurs before the decoupling, the energy is only injected into the neutrino fluid, and the effective number N_ν is increased.

The model is now formally defined, and we have mapped the constraints affecting each region of its parameter space. However, three key challenges remain for making testable predictions. First, a mechanism to provide mass to the vectors must be implemented; solutions near the energy scale at which it is activated potentially depend on the choice. Second, we need to build a solver for the Boltzmann equation system to ensure a full solution to the distributions of particles in all regimes. Finally, we must integrate the obtained thermodynamics and expansion history into a unified cosmological solver to co-evolve them. Once this is implemented, precision datasets as CMB, LSS and BBN will be used to identify viable contributions to ΛCDM parameters as N_ν and H_0 and derive observationally allowed ranges for the coupling constant and the mass of the vector boson.

A Massless case

In this section, we will hint what happens in the massless limit of equation (2.11). In that case, the classical solution for B^0 cannot correspond to the one in (2.13). Using the gauge convention $\partial_0 B_0 = \partial_i B_i$, the equations reduce to:

$$(\partial_0^2 - \nabla^2) B_0 = \rho_c \,, \tag{A.1}$$

$$(\partial_0^2 - \nabla^2) B_i = 0 \,. \tag{A.2}$$

A particular solution can be found using the Green's Function Method, with the propagator given by $G_R(X) = 2\theta(X^0)\delta((X^0)^2 - |\vec{X}|^2)$, and $X^\mu \equiv x^\mu - x'^\mu$. The source consists of the constant commoving charge density, $J^\mu = \rho_c\,\theta(\eta - \eta_\star)\delta^{\mu 0}$, with an intrinsic origin in conformal time for such a term. Therefore, the particular solution can be obtained by performing the convolution of the propagator on the source:

$$\begin{aligned} B^0(x) &= \frac{1}{4\pi}\int d^4x' G(x-x')J(x') \\ &= \frac{2\rho_c}{4\pi}\int_{-\infty}^{\infty} dX^0 \int_{\mathbb{R}^3} d^3X \theta(X^0)\delta((X^0)^2 - |\vec{X}|^2)\theta(\eta - X^0 - \eta_\star) \\ &= \rho_c \int_{-\infty}^{\infty} dX^0 \theta(X^0) X^0 \theta((\eta - \eta_\star) - X^0) \\ &= \rho_c \int_0^{\eta - \eta_\star} dX^0 X^0 = \frac{\rho_c(\eta - \eta_\star)^2}{2} \,. \end{aligned} \tag{A.3}$$

Now we can invoke the gauge fixing again to obtain the spatial component,

$$\partial_i B_i = \rho_c(\eta - \eta_\star) \implies B_i = \rho_c(\eta - \eta_\star) x^i/3 \,, \tag{A.4}$$

This solution respects isotropy. At this stage, a subtlety becomes apparent. We are solving these equations under the assumption of a constant charge density $\rho_c = \text{const.}$, which implies that charges remain fixed at comoving coordinates as the universe expands. However, the force generated by B_i will counteract this scenario at sufficiently large distances from the center $x^i = 0$. A more realistic approach would be to consider the movement of charges that arises from (A.4), which would create fermionic currents, $\bar{\psi}\gamma^i\psi \neq 0$, as well as a non-constant ρ_c. In this scenario, deviations from FLRW must be considered. The treatment that we employed is a first step solution to this complicated situation, and allows us to learn about the implications of the existence of a net charge density in the universe.

The solution of A^μ is consistent with both the gauge fixing and the equations of motion. This solution for the potential generates a non-zero electric field of the form $E_i = \partial_0 B_i = \rho_c x_i$, which wouldn't break homogeneity if all matter in the universe were charged in the same way under this field. The situation is entirely analogous to conventional cosmology, with particles coupling to gravitational induced expansion through the mass: a homogeneous and isotropic universe with this configuration remains perfectly viable. However, the presence of neutral particles breaks homogeneity, as it forces us to select a center, i.e. a point where both charged and neutral particles experience no relative motion due to expansion. At any other location, space expands at different rates for charged versus neutral particles. Thus, in the case of $M_B \neq 0$ only uncharged solutions are allowed by the Cosmological Principle, or, in any case, very tight bounds on the charge density can be placed.

The transition from massless to massive solutions is consistent if the mechanism granting mass comes into play before the introduction of the asymmetry. Imagine this is the case: when the particle is massless, we require the absence of ρ_c, as the coupling g is constant, to grant that the universe is uncharged. Once it acquires mass, there will be no sourcing, and the field will only have thermal solutions. Eventually, the asymmetry will be activated by an external mechanism, and the solution for the B field will transition to the classical charged one.

B Computing amplitudes and rates, some details

In this section, we present a schematic of amplitude calculations under B sourcing and the derivation of production rates.

***B* $\to f\bar{f}$:** it is the simplest of all processes, represented in the left diagram in figure 8. Using the Feynman rules we obtain the amplitude,

$$i\mathcal{M} = igu^s(p_1)\gamma^\mu u^s(p_2)\epsilon_\mu(p_A)\,, \quad (p_A = p_1 + p_2)\,. \tag{B.1}$$

We define the squared amplitude averaging over initial polarization states and summing over the final ones,

$$\overline{|\mathcal{M}|}^2 \equiv \frac{1}{3} \sum_{s,s'=\pm\frac{1}{2}} \sum_{h=0,\pm 1} |\mathcal{M}|^2\,. \tag{B.2}$$

While computing amplitudes it is useful to use the completeness relations derived previously in (2.41) and (2.42), as well as the substitution,

$$\sum_{h=0,\pm 1} \epsilon_\nu^{h\,*}(p_2)\epsilon_\mu^h(p_1) = -\eta_{\mu\nu} + \frac{p_{A,\mu}p_{A,\nu}}{M_B^2}\,. \tag{B.3}$$

After expressing the terms in terms of traces we find,

$$\overline{|\mathcal{M}|}^2 = \frac{g^2}{3}\left(-g_{\mu\nu} + \frac{p_{A,\mu}p_{A,\nu}}{M_B^2}\right) \mathrm{Tr}\left[\left((\not{p}_2 + g\not{B}) - m\right)\gamma^\nu \left((\not{p}_1 - g\not{B}) + m\right)\gamma^\mu\right]\,. \tag{B.4}$$

The modified completeness relations ensure that the resulting momenta are the usual physical ones, $(p_2 + gB)^\mu = (\sqrt{m^2 + |\vec{p}_2|^2}, \vec{p}_2)$, $(p_1 - gB)^\mu = (\sqrt{m^2 + |\vec{p}_1|^2}, \vec{p}_1)$. This was expected; the potential energy increase due to the classical solutions should not affect annihilations. After all, the B-background affects both particles and antiparticles with an opposite contribution, leaving the total energy of the incoming particles as if no coupling existed. After computing the kinematics of this process, one finds,

$$\overline{|\mathcal{M}|}^2 = \frac{4g^2 M_B^2}{3}\left(1 + \frac{2m^2}{M_B^2}\right)\,. \tag{B.5}$$

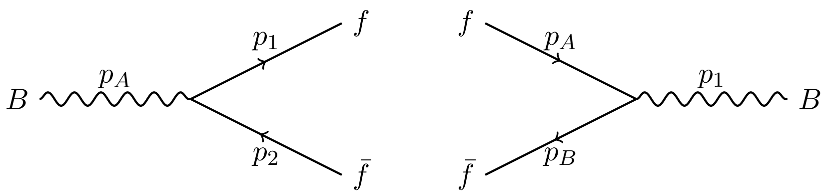

Figure 8. One vertex processes, left: $B \to f\bar{f}$, right: $f\bar{f} \to B$.

Finally, the decay rate can be computed in the center of mass frame:

$$\Gamma_{B\to f\bar{f}} = \frac{\overline{|\mathcal{M}|}^2 |\vec{p}_1|}{8\pi M_B^2} = \frac{g^2 M_B}{12\pi}\left(1+\frac{2m^2}{M_B^2}\right)\sqrt{1-\frac{4m^2}{M_B^2}}\,. \tag{B.6}$$

$\boldsymbol{f\bar{f} \to B}$**:** the amplitude is exactly the same, but the rate cannot be computed directly. First it is needed to obtain the cross-section of the process. The differential cross-section is defined as:

$$d\sigma = \frac{1}{2E_A 2E_B v_{\rm rel}}\frac{d^3p_1}{(2\pi)^3 2E_1}\overline{|\mathcal{M}|}^2(2\pi)^4\delta^4(p_A - p_B - p_1)\,, \tag{B.7}$$

with $v_{\rm rel.} = \left|\frac{\vec{p}_A}{E_A} - \frac{\vec{p}_B}{E_B}\right|$, and after integrating the phase space of the outgoing particle, one finds,

$$\sigma v_{\rm rel} = \frac{1}{2E_A 2E_B}(2\pi)\overline{|\mathcal{M}|}^2\delta((p_A+p_B)^2 - M_B^2)\theta(p_A^0 + p_B^0)\,, \tag{B.8}$$

which corresponds to a narrow transition probability. In order to get an estimation for the value of the cross section we can compute the thermal average, having into account the number of available fermions and antifermions as a function of the temperature. We define it as follows,

$$\langle\sigma v_{\rm rel}\rangle = \frac{1}{n_f n_{\bar{f}}}\int\frac{g_f d^3\vec{p}_f}{(2\pi)^3}\frac{g_{\bar{f}} d^3\vec{p}_{\bar{f}}}{(2\pi)^3} f_f(\vec{p}_f) f_{\bar{f}}(\vec{p}_{\bar{f}})\,(\sigma v_{\rm rel})\,. \tag{B.9}$$

Given the shape of our distribution it is convenient to implement the following change of variables,

$$d^3\vec{p}_f d^3\vec{p}_{\bar{f}} = 2\pi^2|\vec{p}_f|^2|\vec{p}_{\bar{f}}|^2 dE_f dE_{\bar{f}} d\cos\theta = 2\pi^2 E_f E_{\bar{f}} dE_+ dE_- ds \tag{B.10}$$

with $s = (p_1+p_2)^2$, $E_+ = E_f + E_{\bar{f}}$ and $E_+ = E_f - E_{\bar{f}}$. Implementing this change into the average:

$$\begin{aligned}\langle\sigma v_{\rm rel}\rangle = \frac{1}{n_f n_{\bar{f}}}\frac{g_f^2}{2(2\pi)^3}\int_{2m^2}^{\infty} ds\int_{\sqrt{s}}^{\infty} dE_+\int_{-\sqrt{s-4m^2}\sqrt{(E_+^2-s)/s}}^{\sqrt{s-4m^2}\sqrt{(E_+^2-s)/s}} dE_-\times \\ \times f_f(\vec{p}_f) f_{\bar{f}}(\vec{p}_{\bar{f}})\frac{E_f E_{\bar{f}}}{4E_f E_{\bar{f}}}\overline{|\mathcal{M}|}^2\delta(s-M_B^2)\theta(E_+)\,.\end{aligned} \tag{B.11}$$

Integrating out the s one finds the following integral:

$$= \frac{1}{n_f n_{\bar{f}}}\frac{g_f^2\overline{|\mathcal{M}|}^2}{8(2\pi)^3}\int_{M_B}^{\infty} dE_+\int_{-\sqrt{M_B^2-4m^2}\sqrt{(E_+^2-M_B^2)/M_B^2}}^{\sqrt{M_B^2-4m^2}\sqrt{(E_+^2-M_B^2)/M_B^2}} dE_- f_f(\vec{p}_f) f_{\bar{f}}(\vec{p}_{\bar{f}})\,, \tag{B.12}$$

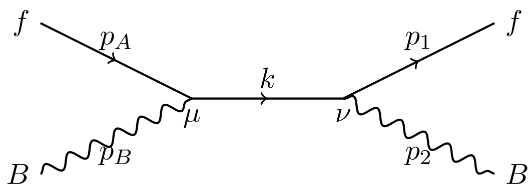

Figure 9. $fB \to fB$ s-channel

that can be computed numerically. Notice that we can extract a rate per volume of such processes as,

$$\frac{\Gamma_{f\bar{f}\to B}}{V} = \langle \sigma v_{\rm rel} \rangle \, n_f n_{\bar{f}} \tag{B.13}$$

and a rate can be estimated by multiplying by the typical scale of such processes, which will be given by the wavelength of the produced particle, $1/\lambda_B = \sqrt{M_B^2 + |\vec{p}|^2} \simeq \sqrt{M_B^2 + T^2}$,

$$\Gamma_{f\bar{f}\to B} = \left(M_B^2 + T^2\right)^{-3/2} \langle \sigma v_{\rm rel} \rangle \, n_f n_{\bar{f}} \,. \tag{B.14}$$

This rates only become relevant at temperatures near the mass of the produced particle, as the phase space is very limited in front of those of other processes.

***fB* → *fB*:** this 2 to 2 process can dominate at high temperatures. We will obtain an estimate of the decay rate for high and low temperatures, doing so by considering only the s-channel for simplicity. Its amplitude is given by,

$$i\mathcal{M}_s = \bar{u}_{s_1}(p_1)(ig\gamma^\mu)\frac{i(\not{k}+m)}{k^2-m^2}(ig\gamma^\nu)u_{s_A}(p_A)\epsilon_\mu^{*\lambda_2}(p_2)\epsilon_\nu^{\lambda_B}(p_B)\,. \tag{B.15}$$

The averaged squared amplitude is,

$$\begin{aligned}\overline{|\mathcal{M}_s|}^2 = \frac{g^4}{6}\left(-g_{\rho\mu} + \frac{p_{2\,\rho}p_{2\,\mu}}{M^2}\right)\left(-g_{\nu\sigma} + \frac{p_{B\,\nu}p_{B\,\sigma}}{M^2}\right) \\ \times \,\mathrm{Tr}\left[(\not{p}_A + m)\gamma^\nu(\not{k}+m)\gamma^\mu(\not{p}_1+m)\gamma^\rho(\not{k}+m)\gamma^\sigma\right]\,.\end{aligned} \tag{B.16}$$

The term that will dominate at high temperatures is the one with the most 4-momenta. This term contains the contribution from the longitudinal mode, provided by the mass of the vector boson. The trace that has to be computed is

$$\mathrm{Tr}\left[\not{p}_A\,\not{p}_B\,\not{k}\,\not{p}_2\,\not{p}_1\,\not{p}_2\,\not{k}\,\not{p}_B\right]\,. \tag{B.17}$$

This trace can be simplified by anticommuting the gamma matrices to combine momenta corresponding to the same particle. As an illustration, consider the following piece:

$$\not{p}_2\,\not{p}_1\,\not{p}_2 = \gamma^\alpha\gamma^\beta\gamma^\delta p_{2\,\alpha}\,p_{1\,\beta}\,p_{2\,\delta} = (-\gamma^\beta\gamma^\alpha\gamma^\delta + 2g^{\alpha\beta}\gamma^\delta)p_{2\,\alpha}\,p_{1\,\beta}\,p_{2\,\delta} \tag{B.18}$$

$$= (-\frac{1}{2}\gamma^\beta\{\gamma^\alpha,\gamma^\delta\} + 2g^{\alpha\beta}\gamma^\delta)p_{2\,\alpha}\,p_{1\,\beta}\,p_{2\,\delta} = -p_2^2\not{p}_1 + 2(p_1\cdot p_2)\not{p}_2\,. \tag{B.19}$$

Through this procedure, the number of gamma matrices within the trace is systematically reduced, yielding a more manageable expression. It is obtained $\overline{|\mathcal{M}|}^2 \simeq \frac{g^4 s^2}{M^4}$, with $s = (p_A + p_B)^2 \propto T^2$. The cross section is given by,

$$\sigma = \frac{1}{64\pi^2 s} \frac{|\vec{p}_i|}{|\vec{p}_f|} \int \overline{|\mathcal{M}|}^2 d\Omega \propto T^2 \,. \tag{B.20}$$

Finally, the decay rate in the massive scenario is given by $\Gamma_{\text{long.}} = \sigma n_f v_{\text{rel.}} \simeq \frac{g^4}{M^4} T^5$. It can be noticed that this is the usual assumption for weak processes in cosmology, identifying the Fermi constant $G_F \propto g^2/M_B^2$. There are also available the transversal modes that give Compton-like contribution $\Gamma_{\text{trans.}} = \frac{g^4}{T^2} n_f v_{\text{rel.}}$, which become relevant at low temperatures and scales above the chiral symmetry recovery. We also take into account the scatterings with antifermions, with the same associated rate.

Acknowledgments

I would like to thank Adrià and Jordi; I thank you for all your feedback, advice, and for all those times you encouraged me to keep moving forward. In short, thank you for everything you've taught me.

To my friends from undergrad and grad school, I want to confess that even if it was physics that set me on this path, step by step, I've realised that the best way to learn was laughing together about how miserable our lives are in the library. I wouldn't be where I am today without you, and I thank you with all my heart.

A la meva familia li dec tot. Gràcies per creure sempre en mi, per donar-me la llibertat de formar-me en aquest camp que m'apassiona i, sobretot, per fer-me sentir que sempre estareu quan ho necessiti. Dono gràcies, Núria, per existir ara i aquí, al teu costat. Gràcies per seguir confiant en què un dia tots dos arribarem allà on sempre hem desitjat.

I a tu avi, et demano disculpes. Disculpa no ser capaç de transmetre't la meva física de la mateixa manera que tu ho feies quan em vas regalar el do de la curiositat, de petit. Tant de bo tothom gaudís de la oportunitat de ser alumne teu.

References

[1] P. J. E. Peebles and Bharat Ratra. The cosmological constant and dark energy. *Reviews of Modern Physics*, 75(2):559–606, April 2003.

[2] Planck Collaboration. Planck2018 results: Vi. cosmological parameters. *Astronomy amp; Astrophysics*, 641:A6, September 2020.

[3] The ATLAS Collaboration. Observation of a new particle in the search for the standard model higgs boson with the atlas detector at the lhc. *Physics Letters B*, 716(1):1–29, September 2012.

[4] Julien Lesgourgues and Sergio Pastor. Massive neutrinos and cosmology. *Phys. Rept.*, 429:307–379, 2006.

[5] Ivan Esteban and Jordi Salvado. Long range interactions in cosmology: implications for neutrinos. *Journal of Cosmology and Astroparticle Physics*, 2021(05):036, May 2021.

[6] Thibaut Louis et al. The Atacama Cosmology Telescope: DR6 Power Spectra, Likelihoods and ΛCDM Parameters. 3 2025.

[7] DESI Collaboration. Desi dr2 results ii: Measurements of baryon acoustic oscillations and cosmological constraints, 2025.

[8] Cristian Moreno-Pulido, Joan Sola Peracaula, and Samira Cheraghchi. Running vacuum in QFT in FLRW spacetime: the dynamics of $\rho_{\rm vac}(H)$ from the quantized matter fields. *Eur. Phys. J. C*, 83(7):637, 2023.

[9] A. O. Barut and I. H. Duru. Exact solutions of the dirac equation in spatially flat robertson-walker space-times. *Phys. Rev. D*, 36:3705–3711, Dec 1987.

[10] Yann Gouttenoire, Geraldine Servant, and Peera Simakachorn. Kination cosmology from scalar fields and gravitational-wave signatures, 2022.

[11] Ilya L. Shapiro. Covariant derivative of fermions and all that, 2022.

[12] Edward W. Kolb and Michael S. Turner. *The Early Universe*, volume 69. Taylor and Francis, 5 2019.

[13] James Alvey, Miguel Escudero, and Nashwan Sabti. What can cmb observations tell us about the neutrino distribution function? *Journal of Cosmology and Astroparticle Physics*, 2022(02):037, February 2022.